Solid Earth Discuss., https://doi.org/10.5194/se-2019-76
Manuscript under review for journal Solid Earth
Discussion started: 8 May 2019

Solid Earth
Discussions
Open Access
EGU

Tempo-spatial variation of the late Mesozoic volcanism in Southeast China testing the western Paleo-Pacific Plate subduction models

Xianghui Li[1, 2 *] Yongxiang Li[1] Jingyu Wang[1] Chaokai Zhang[1] Yin Wang[3] Ling Liu[3]

[1]*State Key Laboratory for Mineral Deposits Research, School of Earth Sciences and Engineering, Nanjing University, Nanjing 210023 China. Email: leeschhui@126.com*

[2]*Institute of Sedimentary Geology, Chengdu University of Technology, Chengdu 610059, China*

[3]*East China Mineral Exploration and Development Bureau, Nanjing 210007, China*

Solid Earth Discuss., https://doi.org/10.5194/se-2019-76
Manuscript under review for journal Solid Earth
Discussion started: 8 May 2019

ABSTRACT

The westward subduction of Paleo-Pacific plate (PPP) played a governing role in tectonic evolution of East Asia. Although various PPP subduction models have been proposed, the subduction age and dynamical process of the PPP remain controversial. In this study, we investigate the geochronology of extrusive rocks and tempo-spatial variations of the late Mesozoic volcanism in Southeast China. We reported zircon U-Pb ages of new 48 extrusive rock samples in the Shi-Hang tectonic zone. Together with the published data, ages of ~300 rock samples from ~40 lithostratigraphic units were compiled, potentially documenting a relatively complete history and spatial distribution of the late Mesozoic volcanism in Southeast China. The results show that the extrusive rocks spanned ~95 Myr (177-82 Ma), but dominantly ~70 Myr (160-90 Ma), with two main age populations of 145-125 Ma and 105-95 Ma. We propose that these ages represent the intervals of the Yanshanian volcanism in Southeast China and the western subduction of the PPP, within which two intensive volcanic eruptional pulses happened. Spatially, the age geographic pattern of extrusive rocks is both the oldest and youngest age clusters occurring in the CZ and the younger intensive group in the SHTB, indicating that the late Mesozoic volcanism migrated northwestly from the coast to the inland prior to ~145 Ma and subsequently retreated southeastly back to the coast. This migration pattern is interpreted to result from a northwestward subduction followed by a southeastward rollback or retreat of the PPP.

Keywords: geochronology; tempo-spatial variation; volcanism; late Mesozoic; Southeast China; Paleo-Pacific Plate

Solid Earth Discuss., https://doi.org/10.5194/se-2019-76
Manuscript under review for journal Solid Earth
Discussion started: 8 May 2019

1. Introduction

It is generally believed that an Andean-type active continental margin had been developed during the late Mesozoic in eastern Eurasia along which the Paleo-Pacific plate (PPP) subducted beneath the East Asia (e.g., Taylor and Hayes, 1983; Faure and Natal'in, 1992; Charvet et al., 1994; Zhou and Li, 2000; Chen et al., 2005; Liu et al., 2017; Li et al., 2019a). The subduction has exerted profound impacts in Southeast (SE) China (e.g., Taylor and Hayes, 1983; Zhou and Li, 2000; Li CL et al., 2014; Li JH et al., 2014; Jiang et al., 2015; Liu et al., 2016;) and many other parts of East Asia (e.g., Stepashko, 2006; Wu et al., 2007; Choi and Lee, 2011; Zhang et al., 2011; Sun et al., 2013; 2015; Dong et al., 2016; Liu et al., 2017), as indicated by the pervasive crustal deformation associated with the Yanshanian orogeny (e.g., Lapierre et al., 1997; Li, 2000; Zhou and Li, 2000) and the widespread magmatism (e.g., Zhou et al., 2006; Sun et al., 2007).

While the overall tectonic setting of the western Pacific in the late Mesozoic is generally accepted, details such as the direction and angle of the PPP subduction remain controversial (e.g., Zhou and Li, 2000; Li and Li, 2007; Sun et al., 2007; Wang et al., 2011; Liu et al., 2012, 2014, 2016; Zheng et al., 2017; Jia et al., 2018). Several tectonic models have been put forward to explain the subduction process or geodynamics. (summary see Jiang et al., 2015; Li et al., 2018). Typical models are: normal subduction (e.g., Lapierre et al. 1997), shallow subduction (e.g., Zhou and Li 2000; Jiang et al. 2009), flat-slab subduction (Li and Li 2007), and subduction initiation in the Permian (e.g., Li and Li 2007 Li et al., 2006; Knittel et al., 2010; Li et al., 2012a, 2012b), Middle Jurassic (e.g., Zhou and Li 2000; Li et al., 2007; Jiang et al. 2009), and Early Cretaceous (e.g., Chen et al. 2008; Liu et al., 2012, 2014). These models were postulated mostly based on the early sparse (bulk K-Ar, Ar-Ar, Rb-Sr) dating data and / or from local and a limited number of samples in each individual article.

One way to test the relevant models is to investigate the spatial and temporal variations of the widespread volcanism during the late Mesozoic in SE China. This effort is facilitated by the existing

Solid Earth Discuss., https://doi.org/10.5194/se-2019-76
Manuscript under review for journal Solid Earth
Discussion started: 8 May 2019

abundant chronological, geochemical, and isotopic data of magmatic rocks from SE China. For the volcanism responded to the PPP subduction, different time intervals and various episodes / cycles / periods of volcanism have been proposed (e.g., Li et al., 1989; Guo et al., 2012; Li CL et al., 2014; Liu et al., 2012, 2014, 2016; Jiang et al., 2015; Ji et al., 2018; Zhang et al., 2018; Yang et al., 2018; Zhang et al., 2019). However, these different views were generally based on separate and often limited datasets that were commonly from only several to a dozen of samples from a local region such as a mining field, or a province, or at most from a relatively wide area of two neighboring provinces. It is essential to obtain spatially more comprehensive datasets from different parts of SE China and also temporally more expanded datasets from sedimentary basin archives that can document the relatively complete volcanic history to achieve a holistic understanding of the late Mesozoic volcanism and geodynamics in SE China.

In this study, we investigate the geochronology of extrusive rocks in the middle and northern Shi-Hang tectonic belt (SHTB. e.g., Gilder et al., 1996; Jiang et al., 2011; Yang et al., 2012). The SHTB contains thick sedimentary strata, which are interbedded with extrusive rocks, and thus has the advantage of providing a more complete stratigraphic archive that preserves more complete and recognizable volcanic events. We also compile the published zircon U-Pb isotope geochronological data of extrusive rocks from the entire SE China. Obviously, ages of the extrusive rocks can constrain the geochronology of the initiation, evolution, and termination of the late Mesozoic volcanism in SE China, i.e. can also help date and better understand the slab subduction between the Asian continent and the PPP in East Asia (e.g., Gilder et al., 1991, 1996). Specifically, we analyze the temporal evolution and the geographical distribution of the late Mesozoic volcanism, whereby the dynamics and process of the PPP subduction can be examined.

2. Geological setting

The South China Block comprises the Yangtze Block and Cathaysia Block. The Yangtze Block has an Archean to Proterozoic basement, whereas the Cathaysia Block has a Proterozoic basement.

Solid Earth Discuss., https://doi.org/10.5194/se-2019-76
Manuscript under review for journal Solid Earth
Discussion started: 8 May 2019

Yangtze and Cathaysia blocks amalgamated during the early Neoproterozoic Orogeny (e.g., Zhao and Cawood, 1999; Wang et al., 2006; Zheng et al., 2007; Li et al., 2009), forming the Jiangnan orogen. A cover sequence of marine strata from the late Neoproterozoic to the Paleozoic was accumulated on the united South China Block that subsequently underwent the Caledonian orogeny (or the Guangxi movement) in the early Paleozoic (e.g., Guo et al., 1989; Qiu et al., 2000; Charvet et al., 2010) and the Indosinian orogeny in the early Mesozoic (e.g., Carter et al., 2001; Lepvrier et al., 2004).

The major Jiangshan-Shaoxing suture zone separating the Yangtze and Cathaysia blocks (e.g., Jiang et al., 2011; Yang et al., 2012) had been reactivated during the Indosinian and Yanshanian movements. During the late Mesozoic Yanshanian, the Andean-type convergent margin was developed along the SE China following the subduction of the PPP. A series of NE-striking back-arc basins associated with widespread and large-scale magmatism were produced (e.g., Zhou and Li, 2000; Li and Li, 2007; Liu et al., 2014, 2016; Xie et al., 2017; Yang et al., 2017). Since the deposition in these basins was concomitant with volcanism, it is fairly common that the sedimentary successions are interbedded with volcanic rocks. On the basis of the abundance of volcanic rocks in the strata, these basins can be grouped into three types (Fig. 1): volcanic (-dominated), volcanic-sedimentary, and sedimentary (e.g., Chen et al., 2005; Shu et al., 2009). These three types of basins are roughly separated by two NE-striking fault zones: the Jiangshan-Shaoxing fault zone and the Zhenghe-Dapu fault zone (Fig. 1). The volcanic basins occur SE to the Zhenghe-Dapu fault zone and were formed on the magmatic arc along the coastline, i.e., the Coastal zone (CZ). The volcanic-sedimentary basins occur in the SHTB confined between the two fault zones, and volcanic rocks are typically interbedded and / or intercalated with sedimentary strata. Nevertheless, the late Mesozoic volcanic rocks are almost absent east to the Yujiang-Yudu fault zone in sedimentary basins and western SHTB basins (Fig. 1).

The large-scale magmatism is evidenced by the occurrence of granitic plutons in both the SHTB

Solid Earth Discuss., https://doi.org/10.5194/se-2019-76
Manuscript under review for journal Solid Earth
Discussion started: 8 May 2019

and the CZ stretching over 1000 km along the coastal SE China. These granitic plutons intruded into the Precambrian basement and the overlying Paleozoic strata during the Middle Jurassic - Early Cretaceous (e.g., Jiang et al., 2011; Yang et al., 2012). The intrusions mainly occur as A-type and / or I-type granitic rocks, and together with huge volcanic rocks, strongly support the model of the western subduction of the PPP (e.g., Zhao et al., 2016; Jiang et al., 2011; Yang et al., 2012; Xie et al., 2017; Yang et al., 2017).

3. Material and methods

A total of 48 extrusive rock samples were collected from about 20 lithostratigraphic formations (supplementary data Table RD1) in 11 basins / regions within the main SHTB to obtain new zircon U-Pb isotope ages (L1-L10 in Fig. 1; supplementary data Figs. RD1-RD3 and Table RD1). The extrusive rock specimens are volcanic and pyroclastic rocks that are interbedded and intercalated with the sedimentary strata, in which sampling horizons and associated lithologies are marked in the supplementary data figures RD4-RD12. These samples were collected from volcanic layers in the main type sections of typical basins in SE China (supplementary data Fig. RD4-RD12). In general, 3-4 rock samples were taken at lower/base, middle and upper/top part when a lithostratigraphic unit has multiple volcanic horizons or a volcanic layer is over 100-200 m thick (see supplementary data Table RD1). The locations of these samples were determined with a GPS device and are marked on the geological maps (supplementary data Figs. RD1-RD3 and Table RD1).

Zircon grains were separated using the conventional heavy liquid and magnetic techniques. Single zircon grains were handpicked and mounted on adhesive tapes, embedded in epoxy resin, and then polished to about half to one-third of their thickness and photographed in both reflected and transmitted light. Cathodoluminescence (CL) images were taken at the State Key Laboratory for Mineral Deposits Research, School of Earth Sciences and Engineering, Nanjing University, to examine the internal structures of single zircon grains before U-Pb isotope analysis.

Solid Earth Discuss., https://doi.org/10.5194/se-2019-76
Manuscript under review for journal Solid Earth
Discussion started: 8 May 2019

LA-ICP-MS, U-Th-Pb analyses of single zircon grains were performed on a Nd of YAG 213 laser ablation system (Agilent 7500a, New Wave Research, U.S.A.) coupled with VG PQ Excell ICP-MS, which is housed in the State Key Laboratory for Mineral Deposits Research, Nanjing University. General ablation time is ca. 60 s and the ablation pit diameter is at 25-35 μm. The ablation repetition rate is 5 Hz with the incident pulse energy of about 10~20 J/cm^2. Calibrations of mass fractionation were made using the index sample GEMOC/GJ (608 Ma). In each experiment, a total of 11 to 21 zircon grains were measured, among which 8 to 18 grains yield concordant age data. Prior to each experiment, the standard GJ-1 and Mud Tank samples were measured. Other measurements follow the methods described by Jackson et al. (2004). Analyses of Mud Tank sample yielded a weighted $^{206}Pb/^{238}U$ age of 726±10 Ma~737±5 Ma (2σ), which is in good agreement with the recommended value (TIMS age =732±5 Ma, Black and Gulson, 1978).

Data reduction, isotope ratio, age calculation, and Pb correction were conducted with the GLITTER software using Zircon 91500 as an external standard. Data processing and plotting were executed with the Isoplot 3.23 programs (Ludwig, 2001). The uncertainties of age results are quoted at 1σ confidence level, whereas errors for weighted mean ages are quoted at 2σ.

It is worth noting that those aged samples of mafic dykes, basalts and gabbros were not herein compiled for the analysis of volcanic temporal-spatial variation in SE China. This is because: 1) among the magmatic rocks, gabbros and basalts are rare, and diorites and andesites are even less common in South China (Zhou and Li, 2000), leading to a weak significance in statistic of the volcanic samples; 2) those published ages of the dykes, basalts and gabbros were mainly measured using different (Ar-Ar, K-Ar, Rb-Sr) isotopic methods (e.g., Li, et al., 1989; Chen et al., 2008b; Wang et al., 2008; Meng et al., 2012), likely causing chaos of real ages; 3) it is difficult to obtain a good isotopic age for mafic rocks, and particularly, the bulk (basalt) samples ages by K-Ar, Ar-Ar, and Rb-Sr are ~ 10-20 Ma younger than those by zircon U-Pb isotopes (Li et al., 2019b); and 4) some basalts are of the Indosinian orogeny age, instead of the Yanshanian orogeny.

Solid Earth Discuss., https://doi.org/10.5194/se-2019-76
Manuscript under review for journal Solid Earth
Discussion started: 8 May 2019

4. Results

4.1 Uncertainty of zircon U-Pb ages

It is necessary to first evaluate the uncertainty of the new age results and other cited age data. The uncertainty depends on three aspects, i.e. origin of zircon, precision, and accuracy (Schoene et al., 2013).

For the origin, all zircons used in this work were microscopically evaluated with CL to ensure that laser ablation positions of zircons are away from the nucleus, cracks, and inclusions. CL images manifest the growth rings. In the concordant 636 zircons of this work, 20 grains (3.1%) are 0.1-1.0 in Th/U ratio, 615 (96.7%) are 1.0-10.0 (Table 1). Th/U ratios of 3539 zircons can be available in the age data from published references. Together with published data and this work, 1766 zircon grains (42.3%) are 0.1-1.0 in Th/U ratio, 2394 grains (57.3%) are 1.0-10.0, 14 grains (0.3%) are > 10.0, and only one is less than 0.1 (Table 1). CL images and Th/U ratios of this work combined the collected data demonstrate that predominant (>99.9%), if not all, zircons are magmatic origin.

Precision and accuracy uncertainties produced during LA-ICP-MS zircon U-Pb dating have been more and more concerned (e.g., Klötzli et al., 2009; Solari et al., 2010; Li et al., 2015) and come from multiple sources, including the isotopic ratio measurements, the fractionation factor calculation using an external standard, the common lead correction, the external standards, and the data reduction (Li et al., 2015). According to the suggested ~4% (2σ) of precision and accuracy (Li et al., 2015), we used the ~2% and ~2-4% (1σ) to evaluate uncertainties of extrusive rock ages.

A total of 48 rock samples were respectively weighed in mean from 636 concordant zircon U-Pb ages in this work (supplementary data Table RD1 and RD2). In the samples, 46 (95.8%) have a <3 million years (Myr) error in 1σ, in which 36 (75%) samples have <2 Myr error in 1σ; 41 samples (85.4%) have <2.0% (error / age) deviation, and 7 (14.6%) have 2-4% deviation (Table 1). Similar percentages of sample error and age deviation are comparative with those single zircons analyzed in this work (Table 1).

Solid Earth Discuss., https://doi.org/10.5194/se-2019-76
Manuscript under review for journal Solid Earth
Discussion started: 8 May 2019

For zircons from the published data, the literature often provides CL images of zircons showing quite similar nature in source and error. For the zircon U-Pb ages from the previous studies, we carefully examine the experiments described in the literature, re-analyze the concordant ages, and eliminate those that are not concordant and / or greater than ~5% in age deviation (error / age) as well as ages with distinct inheritance, which were not discarded by the original authors. This scrutinizing procedure allows us to identify reliable U-Pb age data from 188 volcanic rock samples from the SHTB and from 103 volcanic rock samples from the CZ (supplementary data Table RD2 and RD3). Then, results show that in the combined 291 samples, 246 samples (85.5% = 246/291) are <2 Myr in 1σ error of age and 39 (13.4 %) are 2-4 Myr; and 264 samples (90.7%) are <2.0% age deviation and 25 (8.6%) are 2-4 Myr deviation in age (Table 1). Closely, total concordant single zircons 4639 are similar in percentages of 1σ error and age deviation with the weighed-mean age samples (Table 1).

The above relatively low errors in 1σ and deviation of age indicate that samples of both this and previous work have highly proportional age results (> ~95%) with fine precision.

Systematic biases often dominate uncertainty in comparisons between dating methods and between laboratories (Schoene et al., 2013). For measurements of our zircon samples, the internal systematic 2σ error is less than 3%, which has been verified by reproductive measurements of Mud Tank sample (see Section 3). These systematic biases were mostly met for those zircons from the references. Therefore, small internal systematic 2σ errors allow our zircon date results to be a moderate accuracy in geochronological application.

The internal systematic conditions are same for weighted mean dates of individual samples from both this and previous work (ref. and comp. to supplementary data Table RD1-RD3). Compiled zircons are predominantly single dates generally within less than 2 Myr in 1σ errors (<3% biases) for the Late Jurassic – Early Cretaceous volcanic rocks. The dates are to great degree consistent with the biostratigraphy of pollens-spores, plants, ostracods, and conchostracans in the volcanic-sedimentary

Solid Earth Discuss., https://doi.org/10.5194/se-2019-76
Manuscript under review for journal Solid Earth
Discussion started: 8 May 2019

basins, SHTB (e.g., Chen and Shen, 1982; Sha, 1990; Jiang et al., 1993; Chen, 2000).

In summary, the zircon origin and the age precision and accuracy indicate the sample weighed-mean ages have relatively low uncertainty and they are eligible for investigating the eruption geochronology of extrusive rocks in SE China.

4.2 U-Pb age spectra of extrusive rocks

Spot analyzing results of this work show that 48 samples have a wide range of (concordant $^{206}Pb/^{238}U$) weighed-mean ages from 162 Ma to 92 Ma (green histogram, Fig. 2a), in which four age populations, ~162-150 Ma, ~144-112 Ma, ~112-102 Ma, and ~102-92 Ma, can be observed. In these populations, two peaks of weighted mean ages are regressed as 133.3 ± 1.5 Ma and 97.2 ± 1.1 Ma, respectively (Fig. 2a). In addition, 636 concordant single zircons from the samples show similar wide age range (166 to 92 Ma) with four age populations and two age peaks (Fig. 2a).

Combining our new results with the published age data from the main SHTB (e.g., Wu et al., 2011a, b; Wu and Wu, 2013; Liu et al., 2012, 2014, 2016; Li CL et al., 2014; Li JH et al., 2014; Ma et al., 2016; Wang et al., 2016; Shu et al., 2017. Locations M1-M22, Table RD1 and Fig. 1) yields a similar age pattern (Fig. 2b). A total of 188 rock samples show that the weighed-mean age range from 177 Ma to 92 Ma with four main populations ~162-144 Ma, ~144-128 Ma, ~128-104 Ma, and 104-92 Ma and two age peaks 136.11 ± 0.38 Ma and 100.0 ± 1.0 Ma (Fig. 2b). Also, a total of 2593 single zircons from the SHTB show the concordant $^{206}Pb/^{238}U$ age ranging from 180 Ma to 92 Ma with four age populations and two age peaks 132.07 ± 0.17 Ma and 101.26 ± 0.23 Ma (Fig. 2b).

The published data of 103 rock samples from the CZ (for Locations N1-N21, see Fig. 1 and supplementary data Table RD1 and RD3. Chen et al., 2008; Li et al., 2009; Guo et al., 2012; Li CL et al., 2014; Liu et al., 2012, 2016; Zhang et al., 2018) show a wide weighed-mean ages ranging from 174 Ma to 82 Ma, five main age populations of ~174-150 Ma, ~150-126 Ma, ~126-102 Ma, ~102-92 Ma, and ~92-82 Ma, and two age peaks of 130.96 ± 0.87 Ma and 98.13 ± 0.55 Ma (Fig. 2c), similar

Solid Earth Discuss., https://doi.org/10.5194/se-2019-76
Manuscript under review for journal Solid Earth
Discussion started: 8 May 2019

229 to those from the SHTB (comp. Fig. 2b and 2c). The 1942 single zircons from the 103 samples also
230 display the same range of concordant $^{206}Pb/^{238}U$ ages (Fig. 2c; supplementary data Table RD3) with
231 similar five main age populations (~180-146 Ma, ~146-126 Ma, ~126-102 Ma, ~102-94 Ma, and
232 ~94-76 Ma) and two age peaks (131.04 ± 0.32 Ma and 99.08 ± 0.32 Ma. Fig. 2c).

233 Further combined and optimized age data of 291 extrusive rock samples of over 40
234 lithostratigraphic units in both SHTB and CZ illustrate that sample weighed-mean ages mainly vary
235 between 177 Ma and 82 Ma, which can be classified as five populations: ~178-145 Ma, ~145-125
236 Ma, ~125-105 Ma, ~105-95 Ma, and ~95-82 Ma (Fig. 3). Of the populations, two peaks are at 133.87
237 ± 0.5 Ma (93 samples, 138-130 Ma, MSWD = 3.7) and 98.19 ± 0.47 Ma (25 samples, 100-96 Ma,
238 MSWD = 1.14), respectively. The compilation of age data from all the 4639 concordant single
239 zircons shows that the $^{206}Pb/^{238}U$ ages range between ~180 Ma and ~76 Ma with five populations of
240 ~180-145 Ma, ~145-125 Ma, ~125-105 Ma, ~105-95 Ma, and ~95-76 Ma and two age peaks at
241 132.90 ± 0.14 Ma and 99.86 ± 0.19 Ma (Fig. 3).

242 **5. Discussion**

243 **5.1 Temporal evolution of volcanism**

244 The late Mesozoic extrusive rocks are widespread in SE China and their dating has been
245 conducted extensively. In early times, they have been roughly dated as the (Late) Jurassic and (to the
246 Late) Cretaceous by the confinement of interbedded / intercalated terrestrial fossil-bearing
247 sedimentary strata, and the ages are quite crude. Later on, Rb-Sr, K-Ar, and Ar-Ar dating of
248 bulk-dominated samples yielded ages of ~150-65 Ma with large age uncertainties in the 1980s-1990s
249 (e.g., Hu et al., 1982; Li et al., 1989; Feng et a., 1993; Zhang, 1997), much younger than the earlier
250 rough estimates, and ~10-20 Myr younger than the zircon U-Pb isotope ages on average (Li et al.,
251 2019b).

252 In the recent decade, though zircon U-Pb age data of the igneous rocks have been reported, rock
253 samples in individual references were taken from separate locations resulting in different age

Solid Earth Discuss., https://doi.org/10.5194/se-2019-76
Manuscript under review for journal Solid Earth
Discussion started: 8 May 2019

interpretations of volcanic eruption in SE China, and a relative concurrent viewpoint has not been reached. Multiple volcanic age durations are available at different locations or regions, such as 145-129 Ma, 143-98 Ma, and 140-118 Ma in eastern and northwestern Zhejiang (Liu et al., 2014), 140-88 Ma and 136-129 Ma in southeastern (Liu et al., 2012) and central Zhejiang (Li JH et al., 2014), 168-95 Ma in northeastern Guangdong and southeastern Fujian (Guo et al., 2012), 162-130 Ma from two locations in Fujian (Li et al., 2009), 160-99 Ma from northern Fujian (Liu et al., 2016), and 112-99 Ma from Zijingshan Mineral Field of Fujian (Jiang et al., 2013, 2015). Obviously, these ages are incomplete and intermittent, and cannot individually reveal the age of volcanism in the entire SE China.

To investigate the geochronology of extrusive rocks, we conducted zircon U-Pb age analysis in the SHTB and combined the published data from both SHTB and CZ. Then relatively high precise and representative dating results are obtained in entire SE China: the combined and optimized ages from 291 rock samples (4639 concordant zircons) range from ~177 Ma to ~82 Ma (mainly 160-90 Ma). As we know, the U-Pb isotope ages of zircons represent the cease time of the crystalline zircon formation when volcanic eruption, therefore, we propose that the age range above is an eligible representation for the duration of volcanism in SE China. That means, the volcanism could have initiated at the late Toarcian (~177 Ma) of the late Early Jurassic and terminated at the early Campanian (~82 Ma) of the Late Cretaceous, and it has a ~95 Myr duration, which shows little discrepancy with those of the single zircon ages (Fig. 3). On the other hand, the volcanism occurred chiefly during the interval of the Late Jurassic-Early Cretaceous (160-90 Ma = 70 Myr) when only several samples with ages of pre-160 Ma and post-90 Ma are regarded (e.g., Chen et al., 2007; Guo et al., 2012; Liu et al., 2012). When one considers the relationship of the magmatism originated by the PPP subduction (details see section 5.3), the above age range and duration are also suggested to represent the westward subduction time of the PPP during the Yanshanian orogeny in East and SE Asia.

Solid Earth Discuss., https://doi.org/10.5194/se-2019-76
Manuscript under review for journal Solid Earth
Discussion started: 8 May 2019

It is noted that among the compiled single zircon U-Pb ages of extrusive rocks, the oldest one is from the Maonong Formation (Fm) in Songyang Basin in Zhejiang. The weighted mean age is 177.4 ± 1.0 Ma for the sample MN01 (location M14. Liu et al., 2012). In addition, a weighted mean age of 180 ± 4 Ma from the same horizon (Chen et al., 2007) has also been reported despite that the error is relatively large, up to 6-8 Myr.

Similarly, variable youngest ages of volcanic rocks are reported. The weighted mean age of 82.5 ± 1.0 Ma of the sample ZJ23 (location N2. Chen et al., 2008) from the Taozu section of eastern Zhejiang could be the youngest age. One zircon grain from the section is dated at 74 ± 0.6 Ma and five zircon grains yield concordant ages of 76 ± 0.6 Ma from the same sample (Table RD3. Chen et al., 2008), suggesting that it is possible the termination of volcanism was ~5 Myr younger than 82.5 Ma.

As we can see from section 4.2, five age populations of extrusive rocks were recognized. We herein suggest age populations as corresponding five stages / pulses of volcanism in SE China, and the two populations ~145-125 Ma and ~105-95 Ma could be the intervals of intensive volcanism in SE China, respectively. The most extensively volcanic eruption episode (145-25 Ma) seems to correspond to the period of rapid increase in the magmatic flux of both the Mid-ocean ridge and Large Igneous Provinces (Coffin & Eldholm, 1994) during the late Late Jurassic - early Early Cretaceous (Fig. 4) although the relationship between them remains unclear.

5.2 Spatial pattern of volcanism

Though it is well-known that the late Mesozoic magmatic rocks are widespread in SE China, the previous volcanic distributions are to some degree out of date as those ages contain large errors with low preciseness and accuracy by bulk isotope dating (e.g., Li et al., 1989; Wang et al., 2000; Zhou and Li, 2000; Chen et al., 2008b) and detailed age distribution patterns by precise age constraints have not been outlined yet. To delineate the spatial variation and migration process of the late

Solid Earth Discuss., https://doi.org/10.5194/se-2019-76
Manuscript under review for journal Solid Earth
Discussion started: 8 May 2019

303 Mesozoic volcanism in SE China, we sketched two age distribution maps of extrusive rocks showing
304 the initial and terminal ages of volcanism (Figs. 5 and 6).

305 Firstly, we identified the initial ages of extrusive rocks. The initial age is defined as the earliest
306 age of volcanic eruption in a location, a basin, and / or a region marked as capital letters L, M and N
307 with numbers in figure 1. Three age boundaries ~163 Ma, ~145 Ma, and ~125 Ma are chosen to
308 divide the initial ages into four intervals: 180-163 Ma, 163-145 Ma, 145-125 Ma, and 125-76 Ma,
309 which are somewhat different from the classification of volcanic pulses in section 5.1. Actually, the
310 three age boundaries ordinarily and clearly correspond to those of the Middle and Late Jurassic, the
311 Late Jurassic and Early Cretaceous, and the early and mid-Cretaceous, respectively. We used the
312 boundary age 163 Ma as a separate boundary within the first period of the volcanism because it
313 represents the initiation time of the first Yanshanian orogenic episode in East and SE Asia and the
314 corresponding stratal boundary is marked by an unconformity (e.g., Yu et al., 2003; Shu et al., 2009).
315 The boundary between the Upper Jurassic and the Lower Cretaceous is also represented by a widely
316 observed unconformity (e.g., Yu et al., 2003; Shu et al., 2009) and the intensification of volcanism in
317 SE China (Fig. 3). As there are fewer samples with ages of < 125 Ma and the age boundary at ~125
318 Ma marks the rapid waning of volcanism (Fig. 3), we combined the three periods 125-105 Ma,
319 105-95 Ma, and <95 Ma of volcanism as one initial recognition.

320 Then, isolines ages are drown by the boundary age 163 Ma, 145 Ma, and 125 Ma, separately.
321 Interpolation ages are used to confine the zones when there are no exact ages same as the boundary
322 age occur in the map. Plotting the initial ages in the geographical map shows four zones of volcanism
323 in SE China (Fig. 5). Zone 1 (177-163 Ma) marks areas where initial volcanic eruption locally occurs
324 in the northernmost Guangdong and neighboring southern Fujian and northeastern Fujian in the CZ
325 and at one location of southwestern Zhejiang (M14, Songyang, Liu et al., 2012) in SHTB. Zone 2
326 (163-145 Ma) delineates areas where initial volcanic eruption occurs around Zone 1 in southern and
327 northeastern Fujian in the CZ, and half extends into the SHTB (Fig. 5). Zone 3 (145-125 Ma) defines

Solid Earth Discuss., https://doi.org/10.5194/se-2019-76
Manuscript under review for journal Solid Earth
Discussion started: 8 May 2019

328 regions where initial volcanic eruption chiefly and largely extends in the SHTB and mostly bounded
329 in west of the volcanic area, extending along the eastern Jiangxi, northwestern Fujian, and western
330 Zhejiang (Fig. 5). Zone 4 (125-90 Ma) locally occupies eastern Zhejiang and limited southeastern
331 Fujian in the middle-eastern CZ (Fig. 5). Same zones can be also recognized in the map made from
332 the single zircon U-Pb ages (comp. the supplementary data Fig. RD13), supporting the zonations of
333 the sample weighed-mean ages.

334 Secondly, five populations of 145-135 Ma, 135-125 Ma, 125-115 Ma, 115-95 Ma, and <95 Ma
335 are designed with a 10 Myr interval for the terminal volcanism in SE China, which are slightly
336 different from the initial ages (comp. Figs. 5 and 6). The age interval scheme is helpful to distinguish
337 the terminal volcanic distribution. This is because the main population ages are totally much younger
338 than 145 Ma and few samples are younger than 95 Ma, for which the main population isolines are
339 more readily made.

340 Similarly, isolines ages are drown by the boundary age 135 Ma, 125 Ma, 115 Ma, and 95 Ma,
341 separately, and interpolation ages are used to confine the zones when there are no exact ages in the
342 map. The isolines in the geographical map also shows five age zones for the terminal volcanism in
343 SE China (Fig. 6). Zone 1 (145-135 Ma) sparely occurs in the southern and northeastern Fujian,
344 similar to those of the initial age distribution. Zone 2 (135-125 Ma) mainly occurs in eastern Jiangxi,
345 western SHTB while partly surrounds the Zone 1; Zone 3 (125-105 Ma) distributes in the boundary
346 region of eastern Jiangxi and western Fujian and in middle Zhejiang in the SHTB. Zone 4 (105-95
347 Ma) appears in regions of the southern Fujian, middle Zhejiang in the eastern SHTB and CZ. Zone 5
348 (<95 Ma) sporadically displays in the eastern Fujian, eastern Zhejiang, and northern Guangdong in
349 the CZ. Same zonations can be classified in the map sketched by the single zircon U-Pb ages
350 (supplementary data Fig. RD14), verifying the zones of the sample weighed-mean ages in SE China.

351 Zonations of both initial and terminal volcanism indicate a distinct pattern of volcanic extrusion
352 in SE China (Figs. 5 and 6): the oldest ages in the CZ, the younger intensive age clusters in the

Solid Earth Discuss., https://doi.org/10.5194/se-2019-76
Manuscript under review for journal Solid Earth
Discussion started: 8 May 2019

353 SHTB, and the youngest ones in the CZ. Detailed distributional patterns can be observed: 1) the
354 earliest appearance and earliest disappearance of extrusive rocks dominantly occur in southern and
355 northeastern Fujian in the CZ; 2) the most widespread distribution of 145-125 Ma extrusive rocks are
356 in eastern Jiangxi, western Zhejiang, and western Fujian in the SHTB; 3) the latest appearance and
357 latest disappearance mainly occur in eastern Zhejiang and eastern Fujian in the CZ. In summary, the
358 first appearance (initial volcanism) area is the first disappearance (terminal volcanism) region.

359 It is surprising that the zone 1 and / or 2 of both initial and terminal volcanism look like
360 thermal-dome patterns (Fig. 5 and 6) by exhumation and exposure that may be related to the regional
361 magmatic intrusion, likely misleading the migration of volcanism. However, the distribution pattern
362 is not dome-controlled because: 1) The data are derived from extrusive rocks, instead of intrusive
363 rocks; 2) it is impossible that a crater is over 200-300 km wide in diameter; 3) lots of agglomerates
364 representing craters were observed in a variety of strata at locations / basins out of Zone 1. For
365 instance, these agglomerates are widespread in basins of western Zhejiang (L1~L4; M9~M14),
366 eastern Jiangxi (L5~L7; M16~M18b), and western Fujian (L8~L10, M19~M22).

367 **5.3 Implication for the PPP Subduction**

368 It is accepted that the late Mesozoic (Yanshanian) magmatism was caused by the subduction of
369 the western PPP even though the subduction geodynamics, direction, and angle remain controversial
370 (e.g., Li and Li, 2007; Sun et al., 2007; Liu et al., 2012, 2014, 2016; Duan et al., 2017; Jia et al., 2018)
371 since the early propositions (e.g., Jahn, 1974; Lapierre et al., 1997; Zhou and Li, 2000). In the
372 subduction model, the magmatism was often attributed to the mantle-crust interaction, that is, the
373 geodynamic environment has been commonly regarded as an active continental margin related to the
374 subduction of the PPP under Eurasia (e.g., Engebretson et al., 1985; Maruyama and Seno, 1986;
375 Faure and Natal'in, 1992; Zhou and Li, 2000; Honza and Fujioka, 2004) and / or Northeast Asia (e.g.,
376 Stepashko, 2006; Wu et al., 2007; Choi and Lee, 2011; Zhang et al., 2011; Sun et al., 2013; 2015;
377 Dong et al., 2016; Liu et a., 2017) as well as SE China (e.g., Faure et al., 1996; Chen and Jahn, 1998;

Solid Earth Discuss., https://doi.org/10.5194/se-2019-76
Manuscript under review for journal Solid Earth
Discussion started: 8 May 2019

Zhou and Li, 2000; Chen et al., 2005; Li et al., 2009; Liu et al., 2012, 2014, 2016; Jiang et al., 2013, 2015; Li CL et al., 2014; Li JH et al., 2014; Duan et al., 2017; Hong et al., 2018; Jia et al., 2018; Zhang et al., 2018). Accordingly, the subduction angle (rollback hypothesis) and / or polarity change are the crucial reference to geodynamics.

There are at least six main models put forward to explain the subduction direction and angles. 1) In an early model, a so-called normal subduction of the PPP happened in the late Mesozoic by felsic arc magmatism and continental olivine tholeiites (Lapierre et al., 1997). 2) PPP westward subducted under the Andesite-type active margin in SE China since the Permian (e.g., Li et al., 2006; Knittel et al., 2010; Li et al., 2012; Li et al., 2012). 3) The dip angle of the PPP subduction slab increased (low to median angle) since the beginning of the Early Cretaceous, resulting in oceanward migration of the magmatic zone to the coastal area (Zhou and Li, 2000). 4) A long-lasting, persistent northwestward subduction between ~250 Ma and ~190 Ma with a subsequent retreat between ~180 Ma and ~155 Ma was proposed to explain the development of a broad (~1300-km-wide) intracontinental orogen in South China (Li and Li, 2007). 5) The southwestward then northwestward subducted in the late Mesozoic (180–125 Ma) (e.g., Sun et al., 2007); 6) The shallow subduction and slab rollback took place during the Middle-Late Jurassic and late Early Cretaceous (e.g., Jiang et al., 2009, 2015; He and Xu, 2012; Liu et al., 2014, 2016; Yang et al., 2018; Zhang et al., 2019).

However, these models were mostly based on two situations. One is that the authors mostly employed the dating and geochemical data from unpublished and local reports in the 1980s-1990s, which were mainly measured from (non-zircon) bulk samples using methods and techniques of Ar-Ar, Rb-Sr, and Sm-Nd and others with less precision and accuracy. By the state of art at the time, those data could have led to the misunderstanding of the model. Another situation is that well-dated materials were mainly derived from a local mining field, a region, a province, or at most a boundary area of two or three provinces. These two situations of imprecise ages and local material could have resulted in incompleteness even mistaking on the PPP subduction process.

Solid Earth Discuss., https://doi.org/10.5194/se-2019-76
Manuscript under review for journal Solid Earth
Discussion started: 8 May 2019

To examine the models of the PPP subduction directions and angles, we combined our new zircon U-Pb dating works with lots of published ages and tried to analyze the tempo-spatial variation of the late Mesozoic volcanism in SE China, which may shed new light on the PPP subduction. It is worth noting that the association of the late Mesozoic volcanism in SE China with the western PPP subduction has been demonstrated by numerous geochronological and geochemical studies of both intrusive and extrusive rocks from variable locations (e.g., Yu et al., 2006; Jiang et al., 2011; Guo et al., 2012; Yang et al., 2012; Liu et al., 2012, 2014, 2016; Jiang et al., 2015; Li WX et al., 2017; Shu et al., 2017; Ji et al., 2018; Jia et al., 2018; Zhang et al., 2018). The age data of this study and those compiled from previous work were derived from similar / same basins and / or locations (refer to Fig. 1 and supplementary data Table RD1), indicating the combined data have the same tectonic meaning. That means the extrusive rock samples for age analysis used in this paper are eligible for the linkage of the PPP subduction.

As shown in sections 5.1 and 5.2, zonations of both initial and terminal volcanism can be made by age distribution of the late Mesozoic extrusive rocks, indicating a migration process of volcanic extrusion in SE China. We proposed a volcanic process that took place in the following sequence (Figs. 5, 6, and 7). Firstly, the volcanism occurred in northeastern Fujian and southern Fujian (Zone 1) of the CZ. It is noteworthy that a few zircon U-Pb isotope ages (interval ~195-180 Ma) of the Early Jurassic from southernmost Jiangxi were recently published (e.g., Cen et al., 2016). These ages belong to the late episode of the Indosinian orogeny. It likely indicates that Zone 1 can reach southernmost Jiangxi if its relevance to the Yanshanian movement is verified. Secondly, the magmatic extrusion happened in eastern Jiangxi and southwestern Fujian (Zone 2) in the main SHTB. Then it appeared in northern Fujian and middle Zhejiang (Zone 3) in the SHTB. Finally, the volcanic eruption had been transferred and emerged in eastern Zhejiang and at limited locations in southeastern Fujian (Zone 4-5) in the CZ. The zonation and process of the volcanic extrusion suggest that the volcanism first advanced northwestward and then retreated southeastward during the late

Solid Earth Discuss., https://doi.org/10.5194/se-2019-76
Manuscript under review for journal Solid Earth
Discussion started: 8 May 2019

Mesozoic. The southeastward retreat of volcanism is also indicated by the change of the main interval of intense volcanic extrusions, that is, the first interval (~145-125 Ma) of intensive volcanism mainly occurred in eastern Jiangxi, western Fujian, and middle Zhejiang, indicating a broad volcanism at the time; and the second one (105-95 Ma) mainly appeared in Tiantai area of eastern Zhejiang and Fuqing-Dehua (southwest to Fuzhou) area of eastern Fujian (Figs. 5 and 6), illustrating a constricted volcanism at last.

By the detailed characterization of the temporal and spatial variations of the late Mesozoic volcanism from the much more comprehensive data of geochronology in SE China, we refined and put forward a different single model of the subduction dynamics in western Pacific (Fig. 7). Based on the migration pattern of volcanism (Fig. 5, 6, and 7), we propose that the PPP subducted northwestward during the Middle-Late Jurassic (178-145 Ma. Fig. 7a) and the subduction slab then rolled back or retreated southeastward during the main Early Cretaceous (145-95 Ma. Fig. 7b and 7c). These would have led to the subsequent southeastward retreat of volcanism (Fig. 5) and to the extension of back-arc by lithosphere foundering (Fig. 7b and 7c). The transfer in the migration direction of volcanism from the northwestward to the southeastward may have occurred at ~145 Ma, as evidenced by the great increase in the early Early Cretaceous age population (145-125 Ma) (Fig. 3), implying that the rollback of the PPP may have led to the Early Cretaceous lithospheric extension (e.g., Li, 2000; Chen et al., 2008; Guo et al., 2012; Meng et al., 2012; Shu et al., 2017) and / or the reactivation of the older NE-striking faults (e.g., Wang et al., 2013) in SE China (Fig. 7b and 7c). Indeed, the rollback of the PPP has been proposed previously with the timing ranging from ~190 Ma (e.g., Jiang YH et al., 2015; Cen et al., 2016) to ~90 Ma (e.g., Zhao et al., 2016). But the dominant age interval for the initiation of the PPP rollback was ascribed to the 145-130 Ma (e.g., Li LM et al., 2009; Yang et al., 2012; Li PJ et al., 2013; Li CL et al., 2014; Su et al., 2014; Li et al., 2017; Yang et al., 2018). Combined with the widespread unconformity in SE China (e.g., Yu et al., 2003; Shu et al., 2009), our results from the extrusive rocks indicate that ~145 Ma represents the initiation timing for

453 the rollback of the PPP subduction. Since the beginning of the Late Cretaceous (~ 95 Ma / 105 Ma),
454 the frontier of the PPP may be broken off and a new normal subduction was either re-established or
455 ceased (Fig. 7d). This alternation could have resulted in the fading of the magmatism and caused an
456 unconformity between the gravelly mollase Danxia Supergroup and the underlying Lishui
457 Supergroup in S China (Li et al., 2019b).

458 **6. Conclusions**

459 We analyzed weighed mean ages of 48 extrusive rock samples (total of 636 concordant single
460 zircons) from ~20 lithostratigraphic units at 11 localities in the SHTB. Published ages of 243 rock
461 samples (total of concordant 3662 zircons) from ~40 lithostratigraphic units in SE China are
462 compiled and re-examined. Based on a total of refined 291 sample ages (4639 concordant zircon
463 U-Pb ages) from this study and the published literatures, we propose that the late Mesozoic
464 volcanism in SE China initiated at ~177 Ma (late Toarcian of the late Early Jurassic) and terminated
465 at ~82 Ma (early Campanian of the Late Cretaceous), spanning an ~95 Myr interval (mainly ~70 Myr
466 = 160-90 Ma), during which two peak age populations at 145-125 Ma (the early Early Cretaceous)
467 and 105-95 Ma (the early Late Cretaceous) are interpreted to indicate the two pulses of intensive
468 volcanism. As the volcanism had been associated with the subduction in western Pacific, we suggest
469 that these age range and span represent the time of the Yanshanian subduction of the western PPP in
470 East and Southeast Asia.

471 The spatial change of the late Mesozoic volcanism is used to explore the linkage between the
472 volcanism and PPP subduction. A distinct pattern of volcanic extrusion ages in SE China is found:
473 both the oldest and youngest ages in the CZ and the intensive younger one in the SHTB. The
474 geographical distributions of the volcanic eruption ages reveal a migration process of magmatic
475 extrusion in SE China. The migration scenario of the volcanic extrusion can delineated as: the first
476 zone of volcanism occurred in northeastern Fujian and southern Fujian in the CZ, the second zone
477 moved northwestward to the eastern Jiangxi, western Fujian and western Zhejiang in the western

SHTB; then, the third zone retreated southeastward to the northwestern Fujian and the middle-eastern Zhejiang in the SHTB; Finally, the last zone migrated to the eastern Zhejiang and the middle-eastern Fujian in the CZ.

The tempo-spatial variations of the late Mesozoic extrusive migration indicate that the volcanism first advanced northwestward and then retreated southeastward in SE China. This implies that the PPP probably subducted northwestward during the Middle-Late Jurassic (177-145 Ma) and the subduction slab then rolled back or retreated southeastward during the main Early Cretaceous (145-95 Ma), leading to the subsequent southeastward retreat of volcanism. This change in the migration direction of volcanism from the northwestward to the southeastward happened at ~145 Ma, i.e., beginning of the Cretaceous, probably responsible for the Early Cretaceous lithospheric extension behind the magmatic arc in South China.

Acknowledgments

We thank Ke Cao, Sijing Liang, Yannan Ji, Sihe Wang for participating the field investigation. We are grateful to the reviewers (xxxxxxxx) for their helpful comments and constructive suggestions. This research was supported by National Key R & D Plan (Grant 2017YFC06014005), Natural Science Foundation of China (NSFC) projects 41372106 and 41672097, and National Basic Research Program of China (973 Project) 2012CB822003.

References cited

Black, L. P., and Gulson, B. L.: The age of the Mud Tank carbonatite, Strangways Range, Northern Territory: BMR, J. Aust. Geol. Geophy., 3, 227-232, 1978.

Carter, A., Roques, D., and Bristow, C.: Understanding Mesozoic accretion in Southeast Asia: Significance of Triassic thermotectonism (Indosinian orogeny) in Vietnam, Geology, 29, 211-214, 2001.

Cen, T., Li, W. X., Wang, X. C., Pang, C. J., Li, Z. X., Xing, G. F., Zhao, X. L., and Tao, J. H.: Petrogenesis of early Jurassic basalts in southern Jiangxi Province, South China: Implications for the thermal state of the Mesozoic mantle beneath South China, Lithos, 256-257, 311-330,

2016.

Charvet, J., Lapierre, H., and Yu, Y. W.: Geodynamic significance of the Mesozoic volcanism of southeastern China, J. SE Asian Earth Sci., 9, 387-396, 1994.

Charvet, J., Shu, L. S., Faure, M., Choulet, F., Wang, B., Lu, H. F., and Le Breton, N.: Structural development of the Lower Paleozoic belt of South China: genesis of an intracontinental orogen, J. Asian Earth Sci., 39, 309-330, 2010.

Chen, C. H., Lee, C. Y., and Shinjo, R.: Was there Jurassic paleo-pacific subduction in South China?: constraints from ^{40}Ar-^{39}Ar dating, elemental and Sr-Nd-Pb isotopic geochemistry of the Mesozoic basalts, Lithos, 106, 83-92, 2008b.

Chen, C. H., Lee, C. Y., Lu, H. Y., and Hseh, P. S.: Generation of Late Cretaceous silicic rocks in SE China: Age, major element and numerical simulation constraints, J. Asian Earth Sci., 31, 479-498, 2008.

Chen, C. H., Lin, W., Lan, C. Y., and Lee, C. Y.: Geochemical, Sr and Nd isotopic characteristics and tectonic implications for three stages of igneous rock in the late Yanshanian (Cretaceous) orogeny, SE China, Geol. Soc. Am., Special Paper, 389, 237-248, 2005.

Chen, J. F., and Jahn, B. M.: Crustal evolution of southeastern China: Nd and Sr isotopic evidence, Tectonophysics, 284, 101-133, 1998.

Chen, P. J., and Shen, Y. B.: The Late Mesozoic conchostracan fossils in Jiangsu, Zhejiang and Anhui provinces, Palaeont. Sin. China, 161(17), 2-27 (in Chinese with English abstract), 1982.

Chen, P. J.: The classification and correlation of non-marine Jurassic and Cretaceous of China: Comment. J. Stratig., 24(2), 114-119 (in Chinese with English abstract), 2000.

Chen, R., Xing, G. F., Yang, Z. L., Zhou, Y. Z., Yu, M. G., and Li, L. M.: Early Jurassic zircon SHRIMP U-Pb age of the dacitic volcanic rocks in the southeastern Zhejiang Province determined firstly and its geological significances, Geol. Rev., 53(1), 31-35 (in Chinese with English abstract), 2007.

Chen, W. F., Chen, P. R., Xu, X. S., and Zhang, M.: Geochemical characteristics of Cretaceous basaltic rocks in South China and constraints on Pacific Plate subduction, Sci. China (Series D), 48(12), 2104-2117, 2005.

Choi, T., and Lee Y. I.: Thermal histories of Cretaceous basins in Korea: Implications for response of the East Asian continental margin to subduction of the Paleo-Pacific Plate, Island Arc, 20, 371-385, 2011.

Coffin, M. F., and Eldholm, O.: Large igneous provinces: Crustal structure, dimensions, and external consequences. Rev. Geophy., 32, 1-36, 1994.

Dong, Y., Ge, W. C., Yang, H., Xu, W. L., Zhang, Y. L., Bi, J. H., Liu, X. W.: Geochronology,

geochemistry, and Hf isotopes of Jurassic intermediateacidic intrusions in the Xing'an Block, northeastern China: Petrogenesis and implications for subduction of the Paleo-Pacific oceanic plate. J. Asian Earth Sci., 118, 11-31, 2016.

Duan, G., Chen, H. Y., Hollings, P., Qi, J. P., Xu, C., Zhang, S., Xiao, B., Liu, G. Y., and Liu, J. M.: The Mesozoic magmatic sources and tectonic setting of the Zijinshan mineral field, South China: Constraints from geochronology and geochemistry of igneous rocks in the Southeastern Ore Segment, Ore Geol. Rev., 80, 800-827, 2017.

Engebretson, D. C., Cox, A., and Gordon, R. G.: Relative Motions between Oceanic and Continental Plates in the Pacific Basin, Geol. Soc. Am., Special Paper, 206, 1-59, 1985.

Faure, M., and Natal'in, B.: The geodynamic evolution of the eastern Eurasian margin in Mesozoic times, Tectonophysics, 208, 397-411, doi: 10.1016/0040-1951(92)90437-B, 1992.

Faure, M., Sun, Y., Shu, L. S., and Charvet, J.: Wugong dome extensional tectonics, South China, Tectonophysics, 163(1-4), 77-106, 1996.

Feng, Z. Z.: Mesozoic volcanism and tectonic environments in Fujian, Reg. Geol. China, 4(4), 311-316 (in Chinese with English abstract), 1993.

Gilder, S. A., Gill, J., and Coe, R. S.: Isotopic and paleomagnetic constrains on the Mesozoic tectonic evolution of South China. J. Geophys. Res., 101, 16137-16154, 1996.

Gilder, S. A., Keller, G. R., and Luo, M.: Eastern Asia and the western Pacific timing and spatial distribution of rifting in China, Tectonophysics, 197, 225-243, 1991.

Guo, F., Fan, W., Li, C., Zhao, L., Li, H., and Yang, J.: Multi-stage crust–mantle interaction in SE China: temporal, thermal and compositional constraints from the Mesozoic felsic volcanic rocks in eastern Guangdong-Fujian provinces, Lithos, 150, 62-84, 2012.

Guo, L. Z., Shi, Y. S., Lu, H. F., Ma, R. S., Dong, H. G., and Yang, S. F.: The pre-Devonian tectonic patterns and evolution of South China, J. SE Asian Earth Sci., 3, 87-93, 1989.

He, Z. Y., and Xu, X. S.: Petrogenesis of the Late Yanshanian mantle-derived intrusions in southeastern China: response to the geodynamics of paleo-Pacific plate subduction, Chem. Geol., 328, 208-221, 2012.

Hong, D., Niu, Y. L., Xiao, Y. Y., Sun, P., Kong, J. J., Guo, P. Y., Shao, F. L., Wang, X. H., Duan, M., Xue, Q. Q., Gong, H. M., Chen, S.: Origin of the Jurassic-Cretaceous intraplate granitoids in Eastern China as a consequence of paleo-Pacific plate subduction, Lithos, 322, 405-419, 2018.

Honza, E., and Fujioka, K.: Formation of arcs and backarc basins inferred from the tectonic evolution of Southeast Asia since the Late Cretaceous, Tectonophysics, 384(1-4), 23-53, 2004.

Hu, H. G., Hu, S. L., Wang, S. S., and Zhu, M. Jurassic and Cretaceous age of volcanic rocks on isotope dating, Act Geol. Sin., 56(4), 315-322 (in Chinese with English abstract), 1982.

572 Jackson, S. E., Pearson, N. J., Griffin, W. L., and Belousova, E. A.: The application of laser
573 ablation-inductively coupled plasma–mass spectrometry to in situ U/Pb zircon geochronology,
574 Chem. Geol., 211, 47-69, 2004.
575 Jahn, B. M. Mesozoic thermal events in southeast China, Nature, 248, 480-483,
576 doi:10.1038/248480a0, 1974.
577 Ji, W. B., Lin, W., Faure, M., Chen, Y., Chu, Y., Xu, Z. H.: Origin of the Late Jurassic to Early
578 Cretaceous peraluminous granitoids in the northeastern Hunan province (middle Yangtze
579 region), South China: Geodynamic implications for the Paleo-Pacific subduction, J. Asian Earth
580 Sci., 141, 174-193, 2017.
581 Jia, L. H., Mao, J. W., Liu, P., and Li, Y.: Petrogenesis of the late Early Cretaceous granodiorite –
582 Quartz diorite from eastern Guangdong, SE China: Implications for tectono–magmatic
583 evolution and porphyry Cu–Au–Mo mineralization, Lithos, 304-307, 388-411, 2018.
584 Jiang, S. H., Bagas, L., and Liang, Q. L.: New insights into the petrogenesis of volcanic rocks in the
585 Shanghang Basin in the Fujian Province, China, J. Asian Earth Sci., 105, 48-67, 2015.
586 Jiang, S. H., Liang, Q. L., Bagas, L., Wang, S. H., Nie, F. J., and Liu, Y. F.: Geodynamic setting of
587 the Zijinshan porphyry-epithermal Cu-Au-Mo-Ag ore system, SW Fujian Province, China:
588 constrains from the geochronology and geochemistry of the igneous rocks, Ore Geol. Rev., 53,
589 287-305, 2013.
590 Jiang, W. S., Zhen, J. S., Li, L. T., and Xu, K. D.: Study of the Cretaceous in Zhejiang, China,
591 Nanjing, Nanjing University Press, 1-42 (in Chinese with English summary), 1993.
592 Jiang, Y. H., Wang, G. C., Liu, Z., Ni, C. Y., Qing, L., and Zhang, Q.: Repeated slab advance-retreat
593 of the Palaeo-Pacific plate underneath SE China, Intl. Geol. Re., 57, 472-491, 2015.
594 Jiang, Y. H., Zhao, P., Zhou, Q., Liao, S. Y., and Jin, G. D.: Petrogenesis and tectonic implications
595 of Early Cretaceous S- and A-type granites in the northwest of the Gan-Hang rift, SE China,
596 Lithos, 121, 55-73, 2011.
597 Jiang, Y.H., Jiang, S.Y., Dai, B.Z., Liao, S.Y., Zhao, K.D., and Ling, H.F., 2009, Middle to Late
598 Jurassic felsic and mafic magmatism in southern Hunan Province, Southeast China:
599 implications for a continental arc to rifting: Lithos, vol. 107, p. 185-204.
600 Klötzli U, Klötzli E, Günes Z, and Kosler, J.: Accuracy of laser ablation U-Pb zircon dating: Results
601 from a test using five different reference zircons. Geostand Geoanal Res, 33, 5-15, 2009.
602 Knittel, U., Hung, C. H., Yang, T. F., and Iizuka, Y.: Permian arc magmatism in Mindoro, the
603 Philippines: an early Indosinian event in the Palawan Continental Terrane, Tectonophysics, 493,
604 113-117, 2010.
605 Lapierre, H., Jahn, B.M., Charvet, J., and Yu, Y. W.: Mesozoic felsic arc magmatism and continental

606 olivine tholeiites in Zhejiang Province and their relationship with tectonic activity in SE China,
607 Tectonophysics, 274, 321-338, 1997.
608 Lepvrier, C., Maluski, H., Maluski, H., Van Tich, V., Leyreloup, A., Thi, P. T., and Van Vuong, N.:
609 The Early Triassic Indosinian orogeny in Vietnam (Truong Son Belt and Kontum Massif);
610 implications for the geodynamic evolution of Indochina, Tectonophysics, 393(1-4), 87-118,
611 2004.
612 Li, C. L., Wang, Z. X., Wang, D. X., Cao, W. T., Yu, X. Q., Zhou, G. Z., and Gao, W. L.:
613 Crust-mantle interaction triggered by oblique subduction of the Pacific plate: geochronological,
614 geochemical, and Hf isotopic evidence from the Early Cretaceous volcanic rocks of Zhejiang
615 Province, southeast China, Intl. Geol. Rev., 56(14), 1732-1753, doi: 10.
616 1080/00206814.2014.956347, 2014.
617 Li, J. H., Dong, S. W., Cawood, P. A., Zhao, G. C., Johnston, S. T., Zhang, Y. Q., and Xin, Y. J.: An
618 Andean-type retro-arc foreland system beneath northwest South China revealed by
619 SINOPROBE profiling. Earth and Planet. Sci. Lett., 490, 170-179, 2018.
620 Li, J. H., Ma, Z. L., Zhang, Y. Q., Dong, S. W., Li, Y., Lu, M.A., and Tan. J. Q.: Tectonic evolution of
621 Cretaceous extensional basins in Zhejiang Province, eastern South China: Structural and
622 geochronological constraints, Intl. Geol. Rev., 56(13), 1602-1629, doi:
623 10.1080/00206814.2014.951978, 2014.
624 Li, K. Y., Shen, J. L., and Wang, X. P.: Isotopic geochronology of Mesozoic terrestrial volcanic rocks
625 in Zhejiang, Fujian and Jiangxi China, J. Stratigr., 13(1), 1-13 (in Chinese with English abstract),
626 1989.
627 Li, L. M., Sun, M., Xing, G. F., Zhao, G. C., Zhou, M. F., Wong, J., and Chen, R.: Two late Mesozoic
628 volcanic events in Fujian Province: constraints on the tectonic evolution of southeastern China,
629 Intl. Geol. Rev., 51, 216-251, 2009.
630 Li, P. J., Yu, X. Q., Li, H. Y., Qiu, J. T., and Zhou, X.: Jurassic–Cretaceous tectonic evolution of
631 Southeast China: geochronological and geochemical constraints of Yanshanian granitoids, Intl.
632 Geol. Rev. 55(10), 1202-1219, doi: 10.1080/00206814.2013.771952, 2013.
633 Li, S. Z., Suo, Y. H., Li, X. Y., Zhou, J., Santosh, M., Wang, P. C., Wang, G. Z., Guo, L. L., Yu, S. Y.,
634 Lan, H. Y., Dai, L. M., Zhou, Z. Z., Cao, X. Z., Zhu, J. J., Liu, B., Jiang, S. H., Wang, G., and
635 Zhang, G. W.: Mesozoic tectono-magmatic response in the East Asian ocean-continent
636 connection zone to subduction of the Paleo-Pacific Plate, Earth-Sci. Rev., 192, 91-137, 2019a.
637 Li, W. X., Li, X. H., Wang, X. C., and Yang, D. S.: Petrogenesis of Cretaceous shoshonitic rocks in
638 the northern Wuyi Mountains, South China: A result of the roll-back of a flat-slab?, Lithos,
639 288-289, 125-142, 2017.

Li, X. H. Cretaceous magmatism and lithospheric extension in Southeast China. J. Asian Earth Sci., 18, 293-305. , 2000,

Li, X. H., Li, Z. X., He, B., Li, W. X., Li, Q. L., Gao, Y. Y., and Wang, X. C. The early Permian active continental margin and crustal growth of the Cathaysia Block: in situ U–Pb, Lu–Hf and O isotope analyses of detrital zircons, Chem. Geol., 328, 195–207, 2012a.

Li, X. H., Li, Z. X., Li, W. X., Liu, Y., Yuan, C., Wei, J., and Qi, C. S.: U–Pb zircon, geochemical and Sr–Nd–Hf isotopic constraints on age and origin of Jurassic I- and A-type granites from central Guangdong, SE China: a major igneous event in response to foundering of a subducted flat-slab? Lithos 96, 186-204, 2007.

Li, X. H., Li, Z. X., Li, W. X., Wang, Y. J.: Initiation of the Indosinian Orogeny in South China: evidence for a Permian magmatic arc in the Hainan Island, J. Geol., 114 (3), 341-353, 2006.

Li, X. H., Liu, X. M., Liu, Y. S., Su, L., Sun, W. D., Huang, H. Q., and Yi, K.: Accuracy of LA-ICPMS zircon U-Pb age determination: An inter-laboratory comparison, Sci. China Earth Sci., 58, 1722–1730, doi: 10.1007/s11430-015-5110-x, 2015.

Li, X. H., Zhang, C. K., Li, Y. X., Wang, Y., and Liu, L.: Refined chronostratigraphy of the late Mesozoic terrestrial strata in South China and its tectono-stratigraphic evolution, Gond. Res., 66, 143-167, 2019b.

Li, Z. X., and Li, X. H.: Formation of the 1300-km-wide intercontinental orogen and postorogenic magmatic province in Mesozoic South China: A flat-slab subduction model, Geology, 35, 179-182, 2007.

Li, Z. X., Li, X. H., Chung, S. L., Lo, C. H., Xu, X. S., and Li, W. X.: Magmatic switch-on and switch-off along the South China continental margin since the Permian: transition from an Andean-type to a Western Pacific-type plate boundary,Tectonophysics, 532-535, 271290, 2012b.

Li, Z., Qiu, J. S., and Yang, X. M.: A review of the geochronology and geochemistry of Late Yanshanian (Cretaceous) plutons along the Fujian coastal area of southeastern China: Implications for magma evolution related to slab break-off and rollback in the Cretaceous, Earth-Sci. Rev., 128, 232-248, 2014.

Liu, K., Zhang, J. J., Wilde, S. A., Zhou, J. B., Wang, M., Ge, M. H., Wang, J. M., and Ling, Y. Y.: Initial subduction of the Paleo-Pacific Oceanic plate in NE China: Constraints from whole-rock geochemistry and zircon U-Pb and Lu-Hf isotopes of the Khanka Lake granitoids, Lithos, 274-275, 254-270, 2017.

Liu, L., Xu, X. S., and Xia, Y.: Asynchronizing paleo-Pacific slab rollback beneath SE China: Insights from the episodic Late Mesozoic volcanism, Gond. Res., 37, 397-407, 2016.

Liu, L., Xu, X. S., and Xia, Y.: Cretaceous Pacific plate movement beneath SE China: Evidence from

episodic volcanism and related intrusions, Tectonophysics, 614, 170-184, 2014.

Liu, L., Xu, X. S., and Zou, H. B. Episodic eruptions of the Late Mesozoic volcanic sequences in southeastern Zhejiang, SE China: petrogenesis and implications for the geodynamics of paleo-Pacific subduction, Lithos, 154, 166-180, 2012.

Ludwig, K. R.: Squid 1.02: A User's Manual (2), Berkeley Geochron. Centre, Special Publication, 1-19, 2001.

Ma, Z. L., Li, J. H., Zhang, Y. Q., Dong, S. W., Song, C. Z., and Li, Y.: Geochronological and structural constraints on the lithostratigraphic units of the Lishui Basin, southeastern China, Geol. China, 43(1), 56-71 (in Chinese with English abstract), 2016.

Maruyama, S., and Seno, T.: Orogeny and relative plate motions: example of the Japanese Islands, Tectonophysics, 127, 305-329, 1986.

Meng, L. F., Li, Z. X., Chen, H. L., Li, X. H., and Wang, X. C.: Geochronological and geochemical results from Mesozoic basalts in southern South China Block support the flat-slab subduction model, Lithos, 132-133, 127-140, 2012.

Qiu, Y. M., Gao, S., McNaughton, N. J., Groves, D. I., and Ling, W. L.: First evidence of N3.2 Ga continental crust in the Yangtze Craton of South China and its implications for Archean crustal evolution and Phanerozoic tectonics, Geology, 28(1), 11-14, 2000.

Schoene, B., Condon, D. J., Morgan, L., and McLean, N.: Precision and Accuracy in Geochronology, Elements, 9, 19-24, doi: 10.2113/gselements.9.1.19, 2013.

Sha, J. G. *Plicatounio* from Hekou Formation of Hekou basin, Ninghua, Fujian, with discussion on classification of Plicatounionidae, Acta Palaeont. Sin., 29(4), 472-489 (in Chinese with English abstract), 1990.

Shu, L. S., Zhou, X. M., Deng, P., Wang, B., Jiang, S. Y., Yu, J. H., and Zhao, X. X.: Mesozoic tectonic evolution of the Southeast China Block, New insights from basin analysis, J. Asian Earth Sci., 34, 376-391, 2009.

Shu, X., Yang, S. Y., Jiang, S. Y., and Ye, M. Petrogenesis and geodynamic setting of Early Cretaceous felsic rocks in the Gan-Hang Belt, Southeast China: Constraints from geochronology and geochemistry of the tuffs and trachyandesitic rocks in Shengyuan volcanic Basin, Lithos, 284-285, 691-708, 2017.

Solari, L. A., Gómez-Tuena, A., Bernal, J. P., Pérez-Arvizu, O., and Tanner, M.: U-Pb zircon geochronology with an integrated LA-ICP-MS microanalytical workstation: Achievements in precision and accuracy, Geostand Geoanal Res, 34, 5-18, 2010.

Stepashko, A. A.: The Cretaceous Dynamics of the Pacific Plate and Stages of Magmatic Activity in Northeastern Asia, Geotectonics, 40(3), 225-235, 2006.

Su, H. M., Mao, J. W., Santosh, M., and Xie, G. Q.: Petrogenesis and tectonic significance of Late Jurassic–Early Cretaceous volcanic-intrusive complex in the Tianhuashan basin, South China, Ore Geol. Rev., 56, 566-583, 2014.

Sun, M. D., Chen, H. L., Zhang, F. Q., Wilde, S. A., Dong, C. W., and Yang, S. F.: A 100 Ma bimodal composite dyke complex in the Jiamusi Block, NE China: An indication for lithospheric extension driven by Paleo-Pacific roll-back, Lithos, 162, 317-330, 2013.

Sun, M. D., Xu, Y. G., Wilde, S. A., and Chen H. L.: Provenance of Cretaceous trench slope sediments from the Mesozoic Wandashan Orogen, NE China: Implications for determining ancient drainage systems and tectonics of the Paleo-Pacific, Tectonics, 34, 1269-1289, doi:10.1002/2015TC003870, 2015.

Sun, W. D., Ding, X., Hu, Y. H., and Li, X. H.: The golden transformation of the Cretaceous plate subduction in the west Pacific, Earth-Planet. Sci. Let., 262, 533-542, 2007.

Taylor, B., and Hayes, D.E.: Origin and history of the South China Sea Basin: *in* Hayes, D. E., Ed., The Tectonic and Geologic Evolution of Southeast Asian Seas and Islands: Part 2, Am. Geophys. Union Geophys. Monograph, 27, 23-56, 1983.

Wang, D. Z., Zhou, J. C., Qiu, J. S., and Fan, H. H.: Characteristics and petrogenesis of late Mesozoic granitic volcanic-intrusive complexes in southeastern China, Geol. J. China Uni., 6(4), 487-798 (in Chinese with English abstract), 2000.

Wang, F. Y., Ling, M. X., Ding, X., Hu, Y. H., Zhou, J. B., Yang, X. Y., Liang, H. Y., Fan, W. M., and Sun, W. D.: Mesozoic large magmatic events and mineralization in SE China: Oblique subduction of the Pacific plate, Intl. Geol. Rev., 53, 704-726, doi: 10.1080/00206814.2010.503736, 2011.

Wang, G. C., Jiang, Y. H., Liu, Z., Ni, C. Y., Qing, L., Zhang, Q., and Zhu, S. Q.: Multiple origins for the Middle Jurassic to Early Cretaceous high-K calc-alkaline I-type granites in northwestern Fujian province, SE China and tectonic implications, Lithos, 246-247, 197-211, 2016.

Wang, X. L., Zhou, J. C., Qiu, J. S., Zhang, W. L., Liu, X. M., and Zhang, G. L.: LA-ICPMS U–Pb zircon geochronology of the Neoproterozoic igneous rocks from Northern Guangxi, South China: implications for tectonic evolution, Precambrian Res., 145 (1-2), 111-130, 2006.

Wang, Y. J., Fan, W. M., Cawood, P. A., Li, S. Z.: Sr–Nd–Pb isotope constraints on multiple mantle domains for Mesozoic mafic rocks beneath the South China Block hinterland, Lithos 106, 297-308, 2008.

Wang, Y. J., Fan, W. M., Zhang, G. W., and Zhang, Y. H.: Phanerozoic tectonics of the South China Block: Key observations and controversies, Gond. Res., 23, 1273-1305, doi: 10.1016/j.gr.2012.02.019, 2013.

742 Wu, F., Yang, J., Lo, C., Wilde, S. A., Sun, D., and Jahn, B.: The Heilongjiang Group: a Jurassic
743 accretionary complex in the Jiamusi Massif at the western Pacific margin of northeastern China,
744 Island Arc, 16, 156-172, 2007.
745 Wu, J. H., Liu, F. Y., and Liu, Sh.: SHRIMP U-Pb Zircon Age of Late Mesozoic Trachyte in
746 Xiajiang—Guangfeng and Sannan (Quannan, Dingnan and Longnan)—Xunwu Volcanic Belts,
747 Geol. Rev., 57(1), 125-132 (in Chinese with English abstract), 2011a.
748 Wu, J. H., Xiang, Y. X., and Liu, S.: Wuyi Group of southern Jiangxi and its geological age, J.
749 Stratigr., 35(2), 200-208 (in Chinese with English abstract), 2011b.
750 Wu, J., and Wu, J. H.: Shuangfengling formation in Jiangxi and its geological age, J. East China Inst.
751 Techn., 36, 17-24 (in Chinese with English abstract), 2013.
752 Xie, J. C., Fang, D., Xia, D., Li, Q. Z., and Sun, W. D.: Petrogenesis and tectonic implications of late
753 Mesozoic granitoids in southern Anhui Province, southeastern China, Intl. Geol. Rev., 59(14),
754 1804-1826, doi: 10.1080/00206814.2017.1297964, 2017.
755 Yang, J. B., Zhao, Z. D., Hou, Q. Y., Niu, Y. L., Mo, X. X., Sheng, D., and Wang, L. L.: Petrogenesis
756 of Cretaceous (133–84 Ma) intermediate dykes and host granites in southeastern China:
757 Implications for lithospheric extension, continental crustal growth, and geodynamics of
758 Palaeo-Pacific subduction, Lithos, 296-299, 195–211, 2018.
759 Yang, S. Y., Jiang, S. Y., Zhao, K. D., Jiang, Y. H., Ling, H. F., and Luo, L.: Geochronology,
760 geochemistry and tectonic significance of two Early Cretaceous A-type granites in the
761 Gan-Hang Belt, Southeast China, Lithos, 150, 155-170, 2012.
762 Yang, Y. L., Ni, P., Yan, J., Wu, C. Z., Dai, B. Z., and Yu, Y. F.: Early to late Yanshanian I-type
763 granites in Fujian Province, SE China: Implications for the tectonic setting and Mo
764 mineralization, J. Asian Earth Sci., 137, 194-219, 2017.
765 Yu, X. Q., Shu, L. S., Deng, P., Wang, B., and Zhu, F. P.: The sedimentary features of the
766 Jurassic-Tertiary terrestrial strata in southeast China, J. Stratigr., 27(3), 254-263 (in Chinese
767 with English abstract), 2003.
768 Yu, X. Q., Wu, G. G., Zhang, D., Yan, T. Z., Di, Y. J., and Wang, L. W.: Cretaceous extension of the
769 Gan-Hang Tectonic Belt, southeastern China: constraints from geochemistry of volcanic rocks,
770 Cret. Res., 27, 663-672, 2006.
771 Zhang, B., Guo, F., Zhang, X. B., Wu, Y. M., Wang, G. Q., and Zhao, L.: Early Cretaceous
772 subduction of Paleo-Pacific Ocean in the coastal region of SE China: Petrological and
773 geochemical constraints from the mafic intrusions, Lithos, 334-335, 8-24, 2019.
774 Zhang, C., Ma, C. Q., Liao, Q. N., Zhang, J. Y., and She, Z. B.: Implications of subduction and
775 subduction zone migration of the Paleo-Pacific Plate beneath eastern North China, based on

distribution, geochronology, and geochemistry of Late Mesozoic volcanic rocks, Intl. J. Earth Sci. (Geol Rundsch), 100, 1665-1684, 2011.

Zhang, J. H., Yang, J. H., Chen, J. Y., Wu, F. Y., and Wilde, S. A.: Genesis of late Early Cretaceous high-silica rhyolites in eastern Zhejiang Province, southeast China: A crystal mush origin with mantle input, Lithos, 296-299, 482-495, 2018.

Zhang, L. M.: The Jurassic-Cretaceous boundary in the Zhejiang-Fujian-Jiangxi region, Geol. Rev., 43(1), 25-31 (in Chinese with English abstract), 1997.

Zhao, G. C., and Cawood, P. A.: Tectonothermal evolution of the Mayuan assemblage in the Cathaysia Block: new evidence for Neoproterozoic collisional-related assembly of the South China craton, Am. J. Sci., 299, 309-339, 1999.

Zhao, J. L., Qiu, J. S., Liu, L., and Wang, R. Q.: The Late Cretaceous I- and A-type granite association of southeast China: Implications for the origin and evolution of post-collisional extensional magmatism, Lithos, 240-243, 16-33, doi: org/10.1016/j.lithos.2015.10.018, 2016.

Zheng, W., Mao, J. W., Zhao, H. J., Zhao, C. S., and Yu, X. F.: Two Late Cretaceous A-type granites related to the Yingwuling W-Sn polymetallic mineralization in Guangdong province, South China: Implications for petrogenesis, geodynamic setting, and mineralization, Lithos, 274-275, 106-122, 2017.

Zheng, Y. F., and Zhang, S. B.: Formation and evolution of Precambrian continental crust in South China, Chinese Sci. Bull., 52, 1-12, 2007.

Zhou, X. M., and Li, W. X.: Origin of Late Mesozoic igneous rocks in southeastern China: implications for lithosphere subduction and underplating of mafic magmas, Tectonophysics, 326, 269-287, 2000.

Zhou, X. M., Sun, T., Shen, W. Z., Shu, L. S., Niu, Y. L.: Petrogenesis of Mesozoic granitoids and volcanic rocks in South China: a response to tectonic evolution, Episodes, 29(1), 26-33, 2006.

Solid Earth Discuss., https://doi.org/10.5194/se-2019-76
Manuscript under review for journal Solid Earth
Discussion started: 8 May 2019

800

801 **Tables**

802 Table 1 Percentages of single zircons and rock samples in 1σ error (Myr), error/age ratio, and
803 Th/U ratio of the late Mesozoic extrusive rocks in SE China

Sources	Concordant zircon Number	Rock Sample	1σ error						error/age						Zircon Number (Th/U)	Th/U		
			Age (Myr)	Zircon Number	%	Age (Myr)	Sample Number	%	Ratio	Zircon Number	%	Age (Myr)	Sample Number	%		Ratio	Zircon Number	%
This work in SHTZ	636	48	<3	570	89.6	<2	46	95.8	0-3	581	91.4	<2	41	85.4	636	<0.1	1	0.2
			3-5	63	9.9	2-4	2	4.2	3-5	50	7.9	2-4	7	14.6		0.1-1.0	20	3.1
			>5	3	0.5	>4			>5	5	0.8	>4				1.0-10	615	96.7
																>10	0	0.0
Composed in SHTZ	2593	188	<3	2066	79.7	<2	153	81.4	0-3	2212	85.3	<2	168	89.4	2503	<0.1	1	0.0
			3-5	441	17.0	2-4	31	16.5	3-5	348	13.4	2-4	18	9.6		0.1-1.0	945	37.8
			>5	86	3.3	>4	4	2.1	>5	33	1.3	>4	2	1.1		1.0-10	1543	61.6
																>10	14	0.6
Composed in SHTZ+CZ	4639	291	<3	3543	76.4	<2	246	84.5	0-3	3798	81.9	<2	264	90.7	4175	<0.1	1	0.0
			3-5	898	19.4	2-4	39	13.4	3-5	769	16.6	2-4	25	8.6		0.1-1.0	1766	42.3
			>5	198	4.3	>4	6	2.1	>5	73	1.6	>4	2	0.7		1.0-10	2394	57.3
																>10	14	0.3

804 Notes: Numbers of evaluated zircon grains differ from sources in U-Pb age and Th/U ratio due to unavailability of some original dada. CZ, Coastal zone;
805

Solid Earth Discuss., https://doi.org/10.5194/se-2019-76
Manuscript under review for journal Solid Earth
Discussion started: 8 May 2019

806

807 **Figures**

808

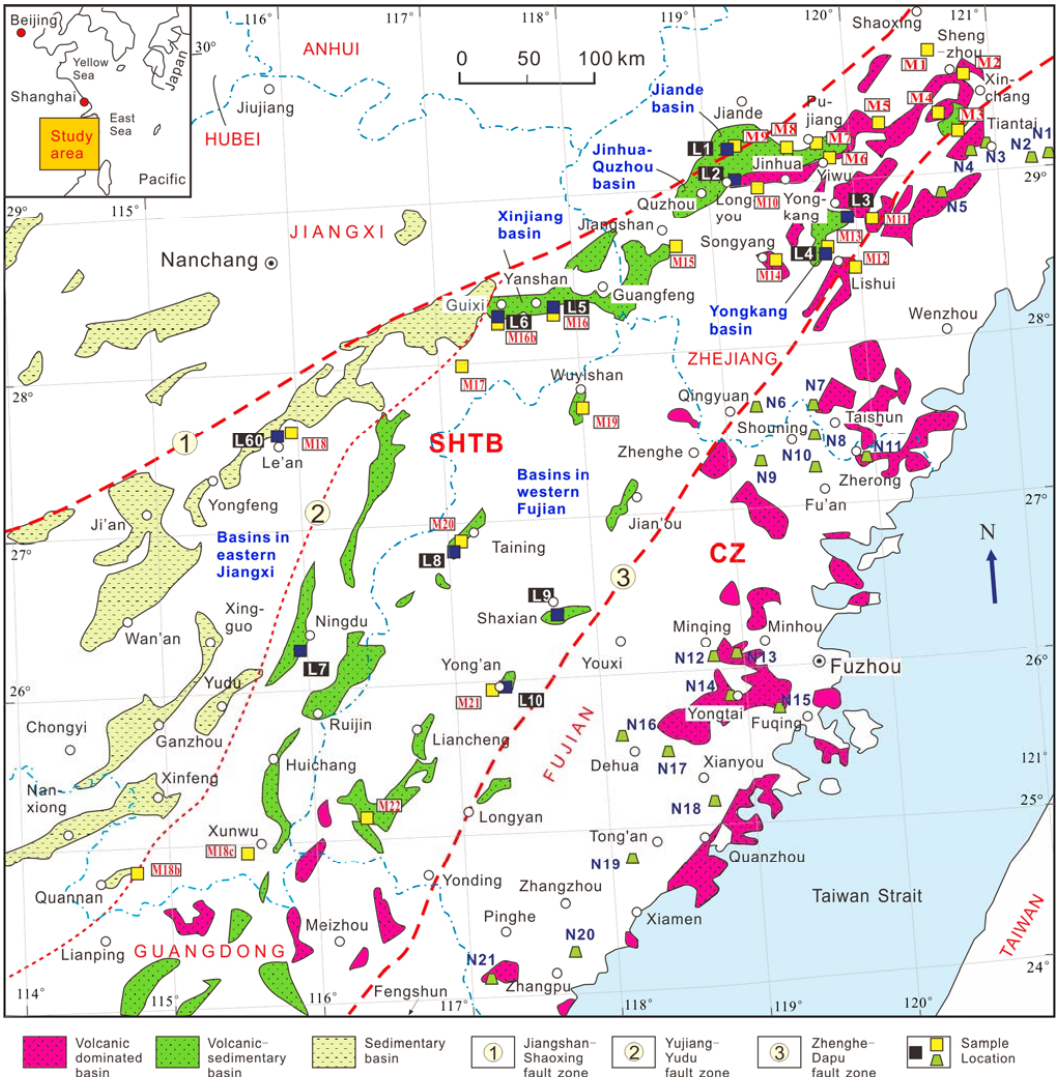

809

810 Figure 1 Sketch geological map of South China showing tectonic and basin zonations of the upper
811 Mesozoic and sample locations (map simplified after Shu et al., 2009). In SHTB (Shi-Hang tectonic
812 belt), dark blue squares with white capital letter L + numbers within black rectangles mark the
813 sampling locations of this study (supplementary data figures RD1, RD2, and RD3), and yellow
814 squares with red capital letter M + numbers within white rectangles indicate sampling locations of
815 previous studies (supplementary data Table RD1 and RD2). In CZ (Coastal Zone), green trapezoids
816 with bold capital letter N + numbers are sample locations of previous studies (supplementary data

Solid Earth Discuss., https://doi.org/10.5194/se-2019-76
Manuscript under review for journal Solid Earth
Discussion started: 8 May 2019

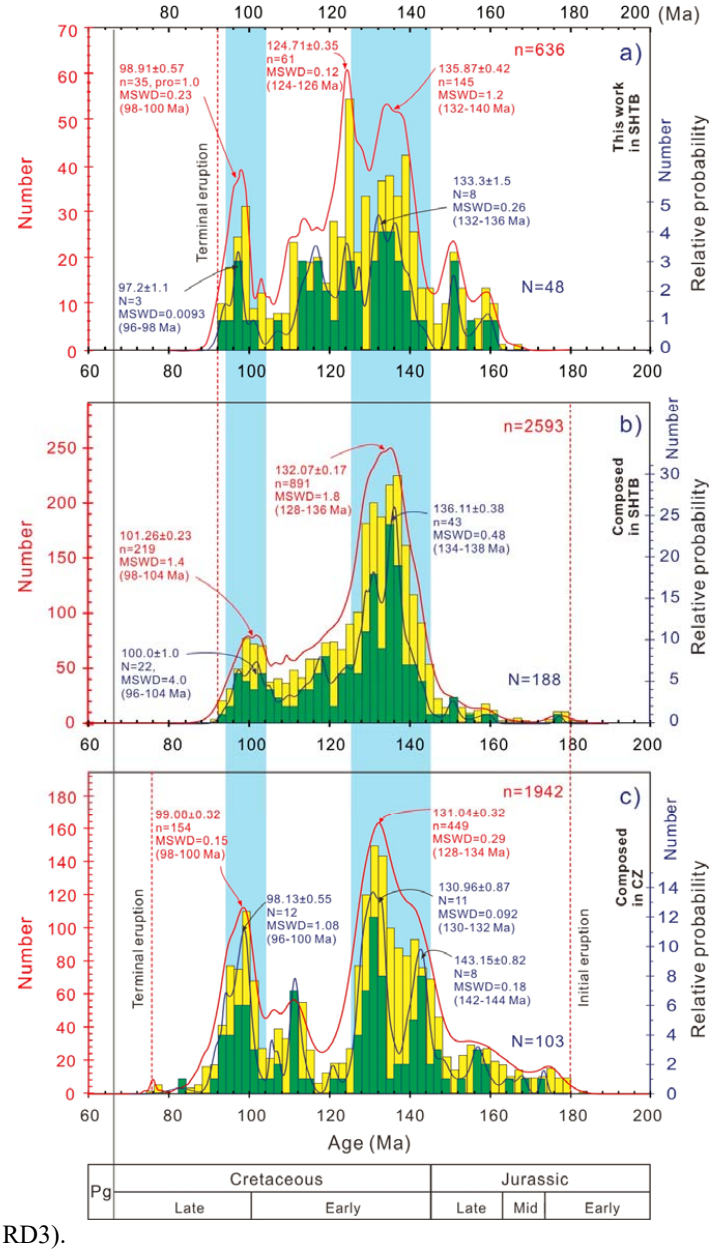

Table RD1 and RD3).

Figure 2 Relative probability and histogram diagrams of concordant zircon U-Pb isotope and sample weighed–mean ages of extrusive rocks from SE China (details see in supplementary data Table RD1, RD2, and RD3). a), this study in the SHTB; b), combined this and previous studies in the SHTB; c), published data in the CZ. N = number of rock samples, n = total number of zircon grains.

Solid Earth Discuss., https://doi.org/10.5194/se-2019-76
Manuscript under review for journal Solid Earth
Discussion started: 8 May 2019

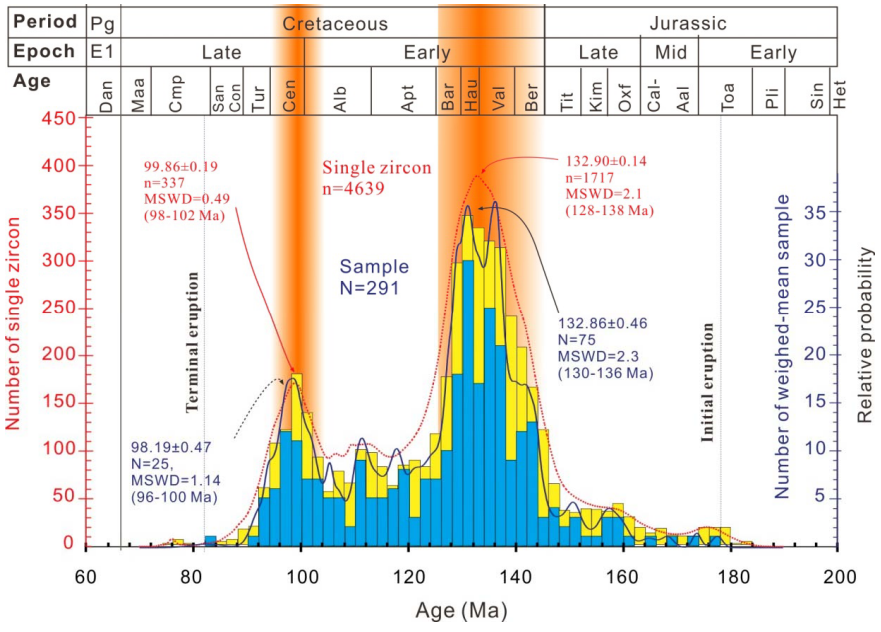

Figure 3 Diagram showing U-Pb isotope age relative probability and histogram of both single zircon and individual sample weighed mean zircons from all extrusive rock samples in SE China. N = number of rock samples, n = total number of zircon grains.

Solid Earth Discuss., https://doi.org/10.5194/se-2019-76
Manuscript under review for journal Solid Earth
Discussion started: 8 May 2019

836

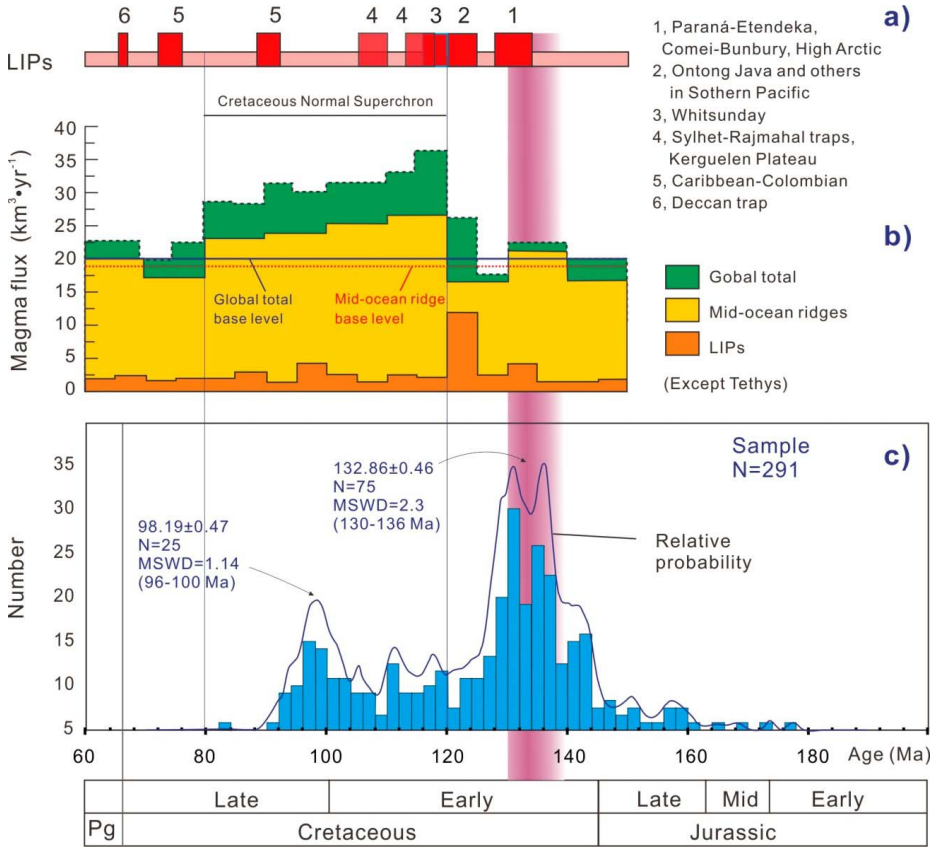

837 Figure 4 Diagram showing age ranges of volcanism in SE China and correlations with the global
838 Large Igneous Provinces (LIPs) and magmatic flux. a, age range of the Cretaceous LIPs (summary
839 see Coffin & Eldholm, 1994); b, magma flux of the Cretaceous LIPs, mid-ocean ridges, and (except
840 Tethys) global total (Coffin & Eldholm, 1994); c, age range of the volcanism with histogram and
841 relative probability and SE China.

842

843

844

845

846

847

Solid Earth Discuss., https://doi.org/10.5194/se-2019-76
Manuscript under review for journal Solid Earth
Discussion started: 8 May 2019

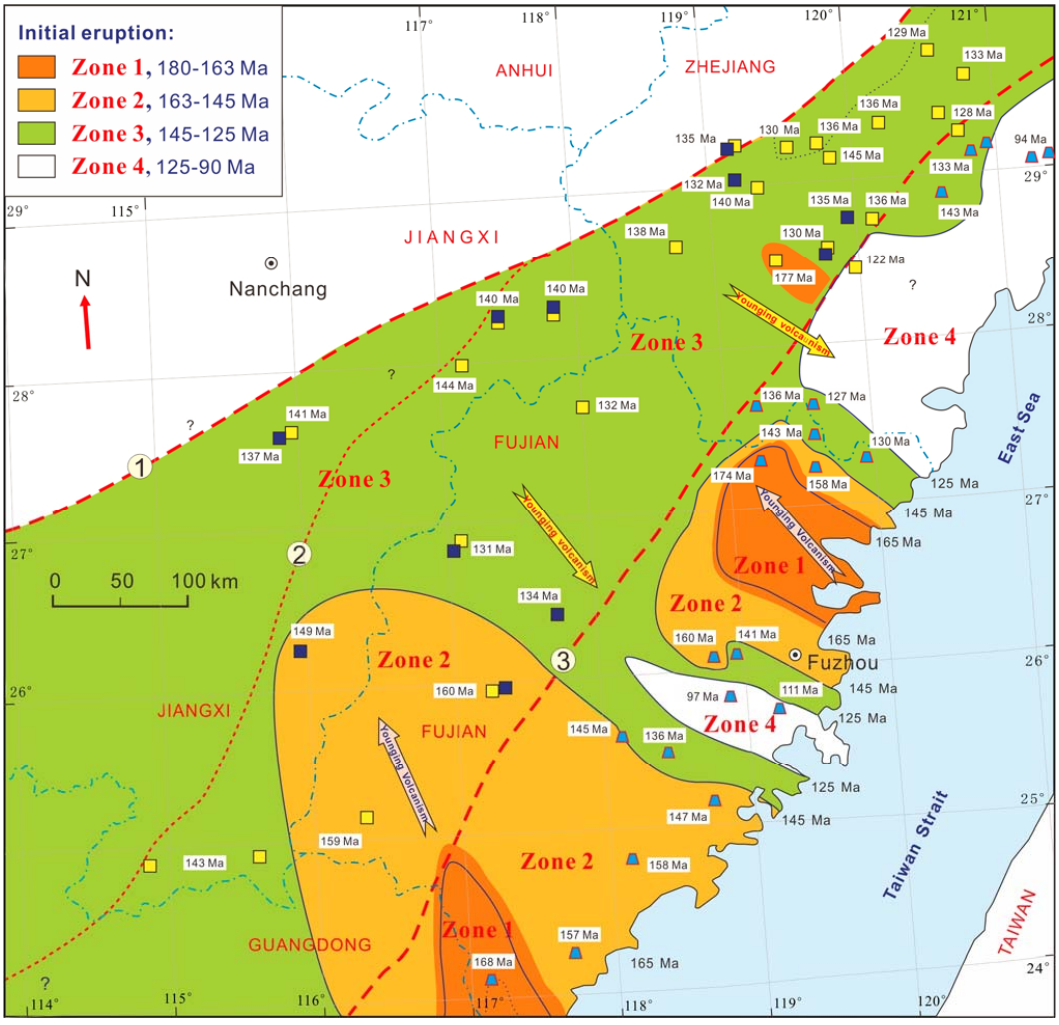

848

849 Figure 5 Sketch map showing extrusive zonations of the late Mesozoic volcanism by initial ages in
850 SE China. Four zonations Zone **1, 2, 3,** and **4** are recognized in the order of the initial eruption age
851 interval 177-163 Ma, 163-145 Ma, 145-125 Ma, and 125-90 Ma, separately. Age within white
852 rectangles is the initial eruption time at a location or in a basin/region. Names of the faults, color
853 squares and trapezoids refer to Fig. 1.

854

855

856

Solid Earth Discuss., https://doi.org/10.5194/se-2019-76
Manuscript under review for journal Solid Earth
Discussion started: 8 May 2019

857

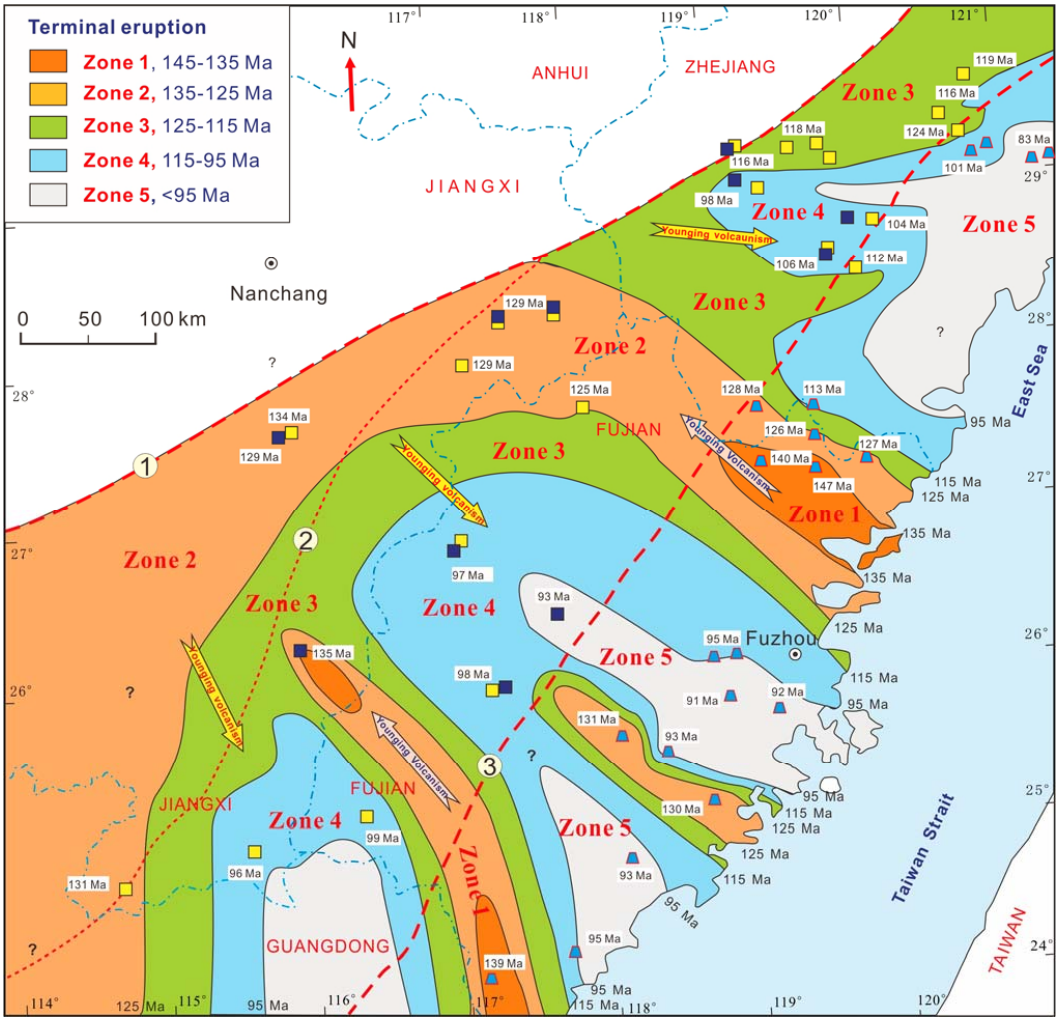

858

859 Figure 6 Sketch map showing extrusive zonations of the late Mesozoic volcanism by terminal ages
860 in SE China. Five zonations Zone **1, 2, 3, 4**, and **5** are recognized in the order of the terminal
861 eruption age interval >145 Ma, 145-125 Ma, 125-115 Ma, 115-95 Ma, and <95 Ma, separately. Age
862 within white rectangles is the terminal eruption time at a location or in a basin/region. Names of the
863 faults, color squares and trapezoids refer to Fig. 1.

864

865

866

Solid Earth Discuss., https://doi.org/10.5194/se-2019-76
Manuscript under review for journal Solid Earth
Discussion started: 8 May 2019

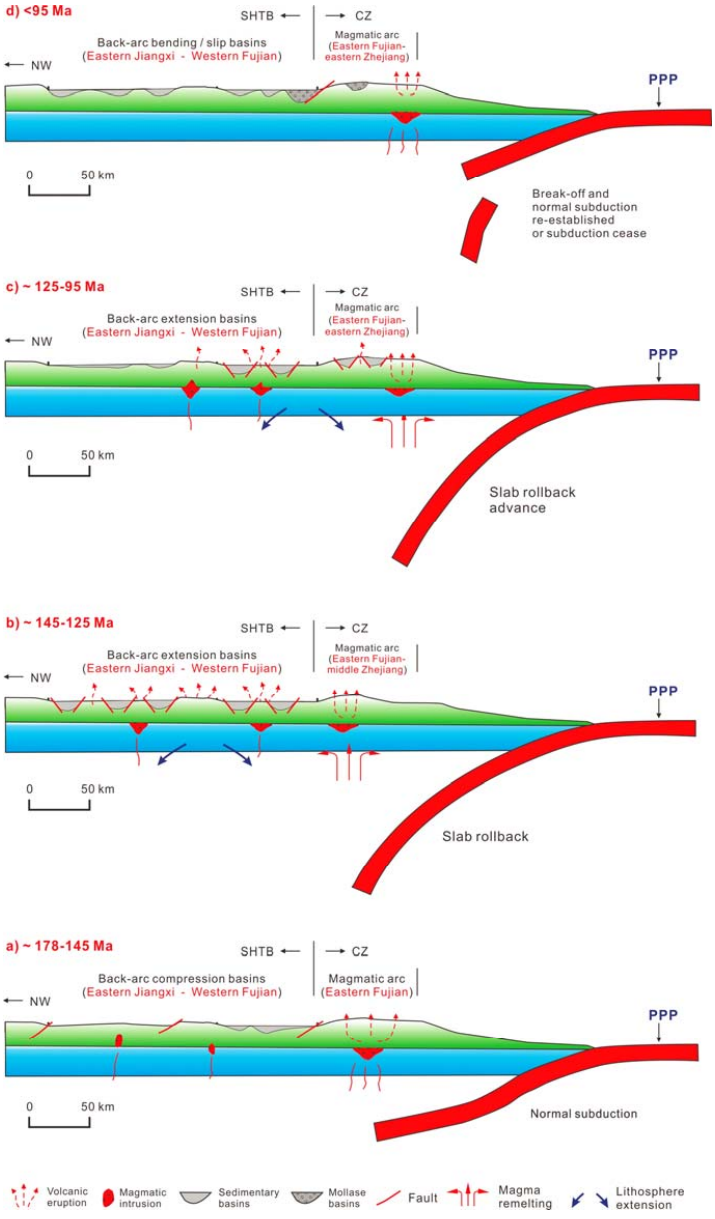

867 Figure 7 Cartoons showing models of the late Mesozoic volcanic advance–retreat and PPP
868 subduction-rollback. a) PPP normal subduction under SE China during the Middle-Late Jurassic
869 (178-145 Ma), during which volcanism chiefly occurred in southern and northeastern Fujian, the
870 magmatic arc (CZ). b) Rollback of the PPP frontier during the early Early Cretaceous (145-125 Ma),
871 leading to the westward volcanism and lithosphere extension in eastern Jiangxi, western Fujian, and
872 middle Zhejiang, back arc (SHTB). c) Rollback advance of the PPP during the late Early Cretaceous
873 (125-95 Ma), resulting in the eastward retreat of volcanism to Fujian and eastern Zhejiang
874 (SHTB-CZ). d) Re-established normal subduction or cease by break-off of the PPP after 95 Ma,
875 fading the magmatism in eastern Fujian and eastern Zhejiang (CZ).